Synthesis and Magnetic studies of pure and doped NiZn ferrite films using Sol gel method

Sushma Kotru,[a,b,*] ,Roni Paul,[a] Jaber Abu Qahouq [a]

[a]*Department of Electrical and Computer Engineering*, [b]*Materials Science Program,*

The University of Alabama, Tuscaloosa, AL 35487, USA

This is the submitted version of the following paper:

Sushma Kotru, Roni Paul, and Jaber Abu Qahouq, "Synthesis and magnetic studies of pure and doped NiZn ferrite films using Sol gel method," Journal of Materials Chemistry and Physics, Volume 276, 15 January 2022. DOI: https://doi.org/10.1016/j.matchemphys.2021.125357

* Corresponding author. Present Address: Electrical and Computer Engineering department, HM Comer Building, 7th Avenue, Tuscaloosa, AL 35487, USA, email: skotru@eng.ua.edu (S. Kotru)

Abstract

In this work, the effect of Co and Cu doping on the magnetic properties of Nickel Zinc ferrite films was investigated. Three types of films with composition $Ni_{0.5}Zn_{0.5}Fe_2O_4$, $Ni_{0.35}Cu_{0.2}Zn_{0.45}Fe_2O_4$ and $Ni_{0.35}Co_{0.2}Zn_{0.45}Fe_2O_4$ were prepared using the sol-gel method. These films were annealed at 500, 600, 700 and 800°C using a rapid thermal annealing furnace. . XRD diffraction confirmed the formation of single-phase spinel structure in these films. Magnetic properties such as saturation magnetization (M_s) and coercivity of these films were measured using an alternating gradient magnetometer. The highest values of M_s were obtained for films annealed at 600 ºC which are 350, 334 and 261 emu/cm^3 for undoped, Co doped and Cu doped films, respectively. The corresponding coercivity values of these films were 102, 509 and 95 Oe. Thus, $Co_{0.2}$ doping resulted in an increase in the coercivity whereas $Cu_{0.2}$ doping reduced the coercivity. Grain size distribution was measured using a scanning electron microscope. It was observed that at higher annealing temperatures (above 600ºC), films developed cracks which results in the reduction of the saturation magnetization from such films.

Key words: Nickel Zinc ferrite, doping, Co, Cu, Sol-gel, Rapid Thermal Annealing, Magnetic properties, Grain Size

1. Introduction:

Nickel–zinc spinel ferrite is of interest due to its low conductivity and high saturation magnetization [1–3] , which makes it suitable for a wide variety of applications including magnetic recording, inductors, and high-frequency microwave devices [4], among many others. Two types of spinel are possible, normal AB_2O_4 and inverse spinel A_2BO_4, where A and B sites represent tetrahedral site and octahedral site, respectively [4]. The magnetic properties depend on the interactions between metallic ions occupying particular positions relative to the oxygen ions in the spinel crystalline structure of the soft ferrites [5]. In the thin film form, various factors including deposition temperature, post growth annealing temperature, and choice of substrate can affect the microstructure of the film, which in turn can affect the film properties [6].

The magnetic properties of Nickel–zinc ferrite vary depending on the grain size, microstructure, type and composition of additives, impurities, and the preparation routes [7]. For bulk NiZn ferrite, it has been shown that the properties can be modified by ion substitution or addition of proper additives like Mn^{2+} [8], Cu^{2+} [9,10], Bi^{3+} [11], W^{6+} [12], and Nb^{5+}[13] ions. Thin films of ferrite have been fabricated by a number of techniques such as spin–spray ferrite plating [14,15], RF sputter deposition [16–19], chemical vapor deposition [20,21], laser ablation techniques [22] and Sol–gel [23–25]. Each processing technique has its advantages and disadvantages. Sol-gel, which is a popular growth technique in piezoelectric and ferroelectric community, is gaining interest in the magnetic community due to low processing temperature and low cost.,

Although there is some literature available on the preparation of Nickel–zinc ferrite films using sol gel, a good understanding on how doping affects the properties of Nickel–zinc ferrite films is still missing. Copper doping has been reported to tune the magnetic properties which could be used

to fabricate multilayer chip inductors and electromagnetic interference filters [26,27]. Properties of Cu- substituted Nickel–zinc films were investigated by Liu et al who reported magnetization value of 271 emu/cc for these films [28]. Structure and magnetic properties of Co-substituted films $\{Ni_{0.5}Zn_{0.5}Co_xFe_{2x}O_4\ (0\leq x\leq 0.2)\}$ synthesized by the sol–gel method was reported by Li et al [29]. Singh et al. reported Cr^{3+} substitution in nickel ferrite films and studied the electro catalytic properties [30]. Liu et al reported crystallographic and magnetic properties of Sn-substituted NiZn ferrite films [31]. The aim of this study is to understand the effect of Co and Cu substitution in NiZn ferrite films prepared by Sol gel and study the co-relation of post growth annealing temperature on the morphology and magnetic properties of these films.

2. Experimental Methods

2.1 Solution Preparation

The precursor solutions with compositions (here after referred as "Sol") of $Ni_{0.5}Zn_{0.5}Fe_2O_4$ (NZF), $Ni_{0.35}Co_{0.2}Zn_{0.45}Fe_2O_4$ (NCoZF) and $Ni_{0.35}Cu_{0.2}Zn_{0.45}Fe_2O_4$ (NCuZF) were prepared in house using chemical solution deposition-sol gel method. To prepare a "Sol" of NZF, high purity salts of Nickel acetate tetrahydrate $\{Ni(OCOCH_3)_2\cdot 4H_2O\}$ (99 % pure from Acros Organics), Zinc acetate dihydrate $\{Zn(CH_3COO)_2.2H_2O\}$ (97% pure from Alfa Aesar), and Iron nitrate nonahydrate $\{Fe(NO_3)_3.9H_2O\}$ (99 % pure from Acros Organics) were used as starting materials. The amount of chemicals used was calculated based on the stoichiometric composition of $Ni_{0.5}Zn_{0.5}Fe_2O_4$ and the desired molarity of the solution. These raw materials were first fully dissolved in dimethylformamide. The solution was stirred for 1 h before acetic acid was added to adjust the concentration of the solution to 0.5mol/L. The solution was again stirred for 2 h, and then left undisturbed (at room temperature) for at least 36 h to form a stable "Sol." The process is summarized in the flowchart of Figure 1. The same process was used to prepare the other two

"Sols" of NCoZF and NCuZF, with the only exception that cobalt nitrate hexahydrate {$Co(NO_3)_2 \cdot 6H_2O$} (98-102% pure from Alfa Aesar) and Copper nitrate trihydrate {$Cu(NO_3)_2.3H_2O$} (Alfa Aeasar) were added respectively as starting materials. In addition, for NCuZF, $(Ni(NO_3)_2.6H_2O$ was used in place of $Ni(OCOCH_3)_2 \cdot 4H_2O$.

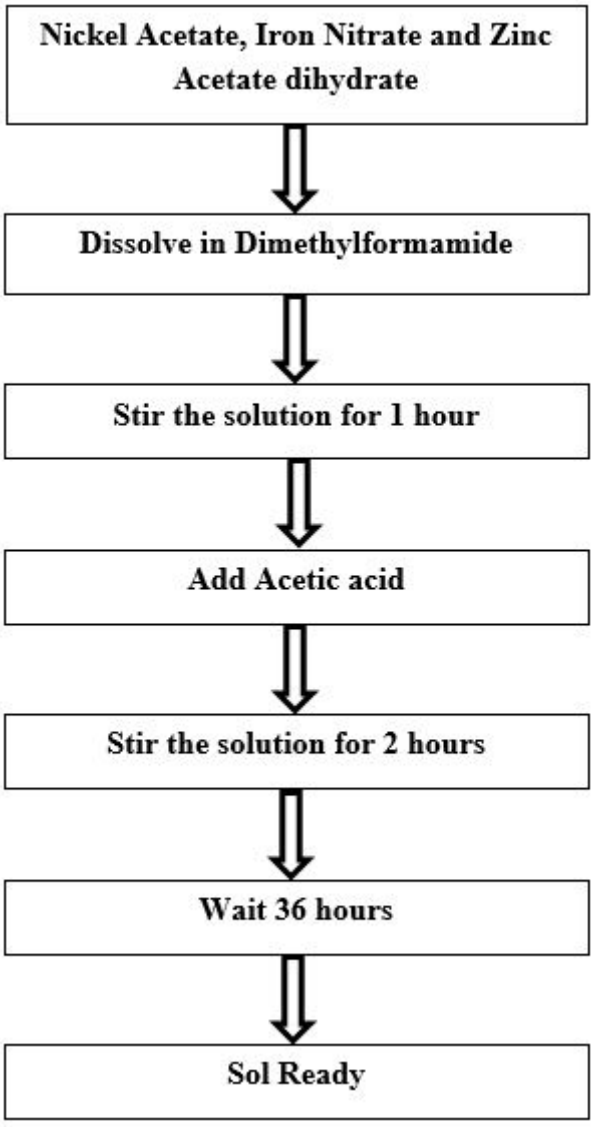

Fig. 1. Flowchart showing the steps for preparing Sol for $Ni_{0.5}Zn_{0.5}Fe_2O_4$

2.2 Film preparation

Using the "Sols" prepared in house, films of $Ni_{0.5}Zn_{0.5}Fe_2O_4$ (NZF), $Ni_{0.35}Co_{0.2}Zn_{0.45}Fe_2O_4$ (NCoZF) and $Ni_{0.35}Cu_{0.2}Zn_{0.45}Fe_2O_4$ (NCuZF) were prepared on Si/SiO_2 substrates using spin coating method. Spin coating method is simple, low cost, and allows deposition of films with uniform thickness over a larger area which is advantageous for scalability. A rotation speed of 4000 rpm and spinning time of 50 s were used for depositing all the films. After depositing each layer, the film went through a hydrolysis step (120 ºC for 30 min on hotplate) to remove the solvents followed by a Pyrolysis step (400 ºC for 30 min on hotplate) to exclude the organic substances [28]. For each film, multiple layers were deposited by repeating the process above until a desired film thickness was obtained. A flowchart showing the films preparation steps and process parameters is presented in Figure 2. The as grown films were amorphous. To promote crystallization, the films were annealed post growth at different temperatures (500, 600, 700, 800 °C) in rapid thermal annealing furnace (RTA) in 2000 sccm of flowing O_2. Annealing temperatures below 500 °C were not used to avoid the formation of intermediate phases of Fe_2O_4 which can be detrimental to magnetic properties [28].

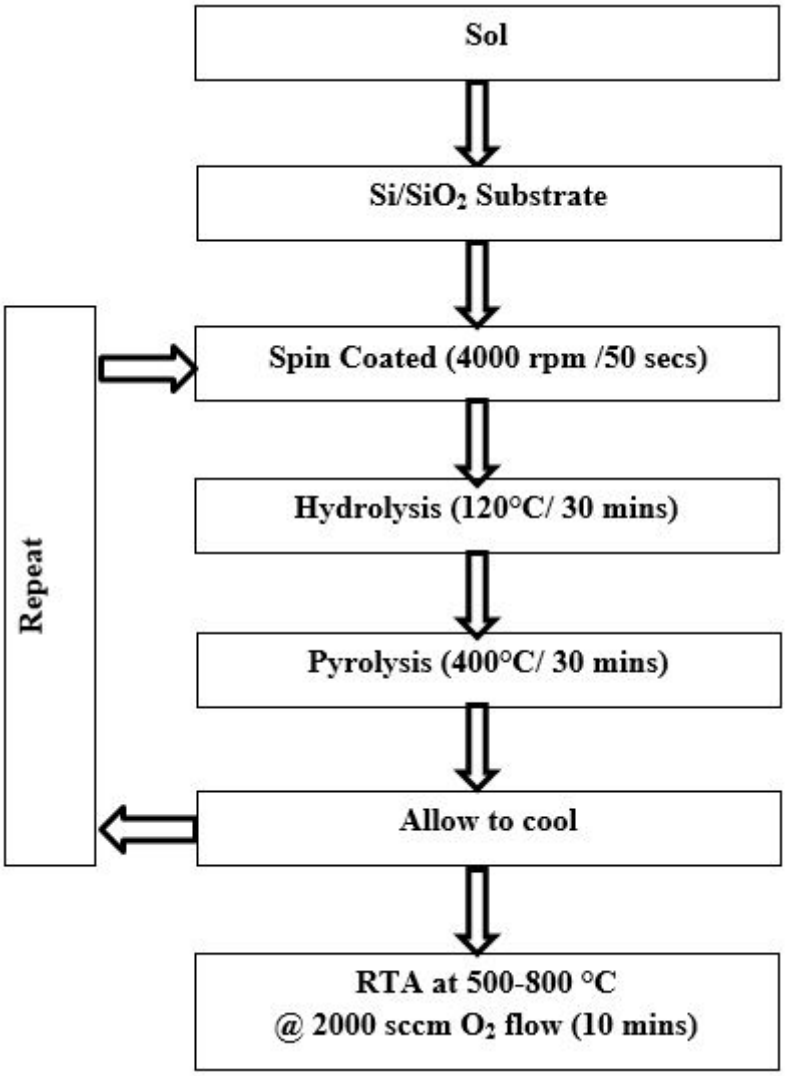

Fig. 2. Flowchart showing the process for film preparation: Sol of NZF, NCoZF and NCuZF were used to prepare the respective films

2.3 Characterization

The XRD diffraction patterns were obtained using Bruker D8 Discover XRD with a Cobalt source as an X-ray generator. The 2θ values were converted from Co source to equivalent Cu source. The surface morphology of the films was observed using Apreo FE-SEM scanning electron microscope (SEM). Grain size was also calculated using SEM. The magnetic properties of the

films were measured at room temperature using an alternating gradient magnetometer (AGM). The maximum applied field was 18 kOe which was applied in increments of 33 Oe. To investigate the effect of post annealing temperature on the magnetic properties of NZF, NCoZF, and NCuZF, each film was cut into four pieces and annealed at 500, 600, 700 and 800 °C for 10 min, resulting in a set of 12 films [28]. The in-plane magnetizations loops were recorded for all samples and the values of saturation magnetization (M_s) and coercivity (H_c) were extracted.

3. Results and Discussions

XRD analysis was performed on NZF, NCoZF and NCuZF films annealed at 600 and 800 °C and the results are presented in Figure 3. For NZF films, the peaks were identified as (111), (220), (311), (222), (440), (422), (333) and (440) by comparing with ICDD-00-069-0240 data. For NCoZF and NCuZF films, (111), (220), (311), (222), (440), (422), (511) and (440) peaks were identified by comparing the data with the ICDD-04-023-9163 and ICDD-04-020-7944. All the peaks match well with the characteristic reflections of cubic spinel structure of NZF, NCoZF and NCuZF and with reported literature [32, 33, 26] confirming absence of any intermediate phases in all the films.

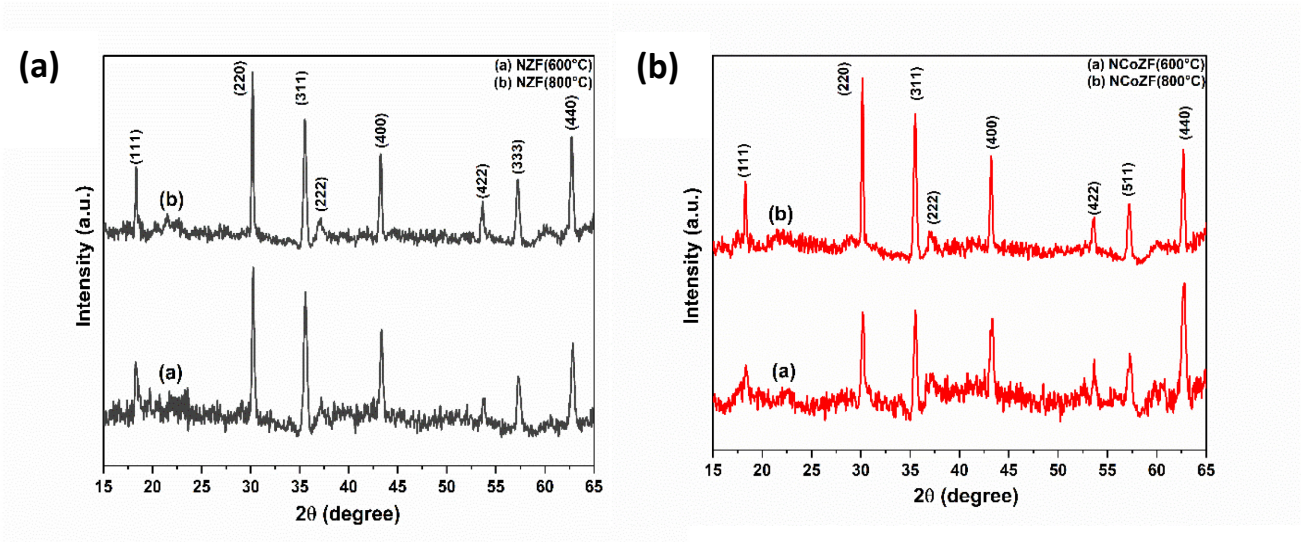

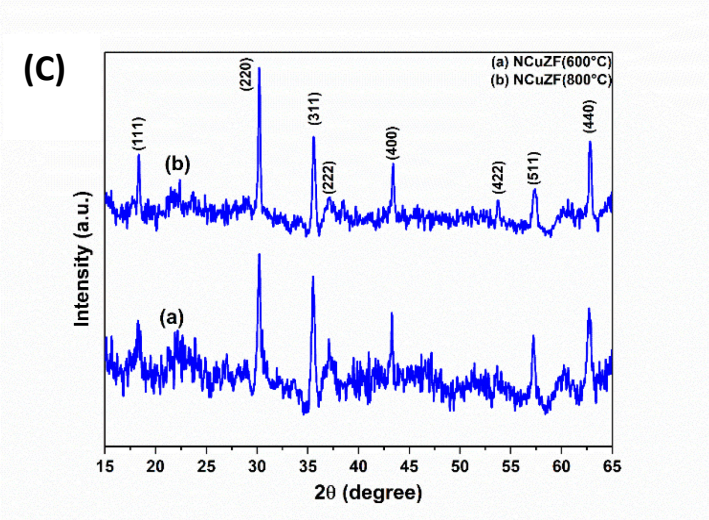

Fig. 3. X-ray diffraction patterns of (a) NZF, (b) NCoZF, and (c) NCuZF films annealed at 600 °C and 800 °C.

The temperature dependence of saturation magnetization (M_s) for NZF, NCoZF and NCuZF films is presented in Fig 4(a). The values for saturation magnetization (M_s) for all the films increased until annealing temperature of 600 ºC and then decreased. The M_s values increased from 256 to 350 emu/cm^3 for undoped NZF films; from 251 to 334 emu/cm^3 for NCoZF films and from 237 to 261 emu/cm^3 for NCuZF, when the annealing temperature increased from 500 to 600 ºC. For films annealed at temperatures higher than 600 ºC, the M_s values decreased in all of the sample types. In general, post growth annealing of films is expected to reduce the amorphous phase, improve crystallinity and consequently improve the saturation magnetization [34]. Accordingly, films annealed at 800 ºC should have resulted in highest values for the saturation magnetization. The reduction in magnetization from films annealed at 800 °C, can be attributed to the enhancement of the (220) peak and reduction in (311) peak intensity for the films annealed at 800 °C in compassion to films annealed at 600 °C as seen from the XRD results.

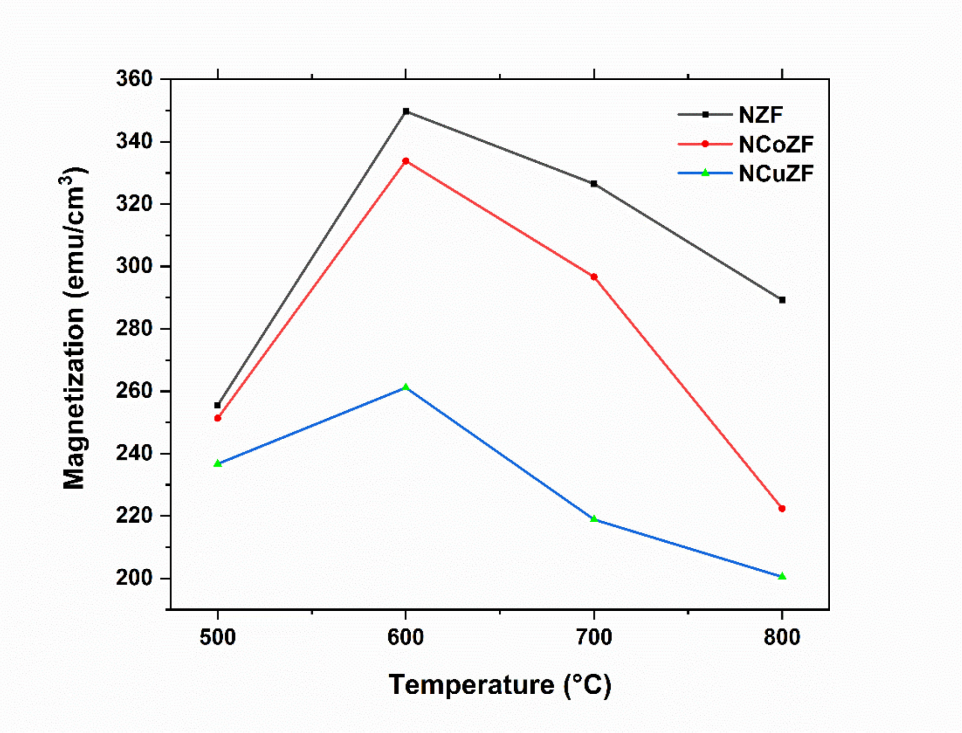

Fig. 4a. Saturation magnetization as a function of annealing temperature for NZF, NCoZF, and NCuZF films

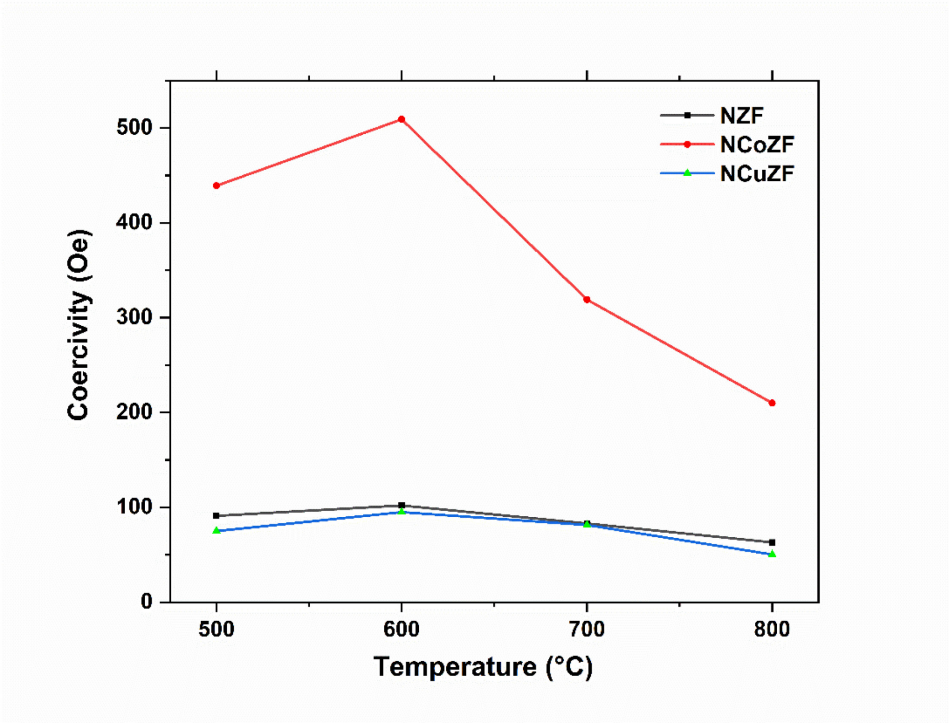

Fig. 4b. Coercivity as a function of annealing temperature for NZF, NCoZF and NCuZF films

A similar trend was seen in the Coercivity (H_c) of these films. The temperature dependence of coercivity (H_c) for NZF, NCoZF and NCuZF films is presented in Fig 4(b). H_c values increased from 91 to 102 Oe for undoped NZF films; from 439 to 509 Oe for NCoZF films; and from 75 to 95 Oe for NCoZF film, when the annealing temperature increased from 500 to 600 ºC. Beyond this temperature, a decreased in H_c values was seen for all the samples. The M_s and H_c values for all the films are summarized in Table I. Among all these films, highest saturation magnetization was obtained for films annealed at a temperature of 600 ºC. A similar behavior from NiZn ferrite films has been reported by Bae. et al. reported [35].

Table I: Saturation magnetization (M_s), remanent magnetization (M_r) and coercivity (H_c) of NZF, NCoZF and NCuZF films annealed at 500, 600, 700 and 800 ° C

Sample	**M_s (emu/cm^3)**				**M_r (emu/cm^3)**				**H_c (Oe)**			
	500 °C	**600 °C**	**700 °C**	**800 °C**	**500 °C**	**600 °C**	**700 °C**	**800 °C**	**500 °C**	**600 °C**	**700 °C**	**800 °C**
NZF	256	350	326	289	70	101	110	106	91	102	83	63
NCoZF	251	334	297	222	107	144	135	95	439	509	319	210
NCuZF	237	261	219	200	46	73	68	53	75	95	81	50

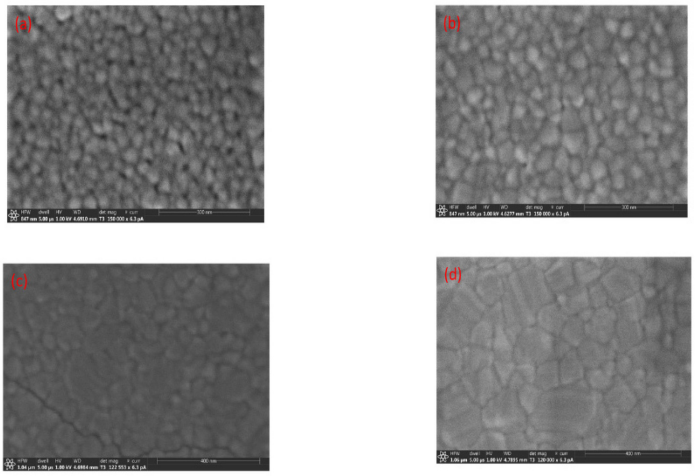

Fig. 5. Surface morphology of NZF films annealed at (a) 500ºC (b) 600ºC(c) 700ºC and (d) 800ºC

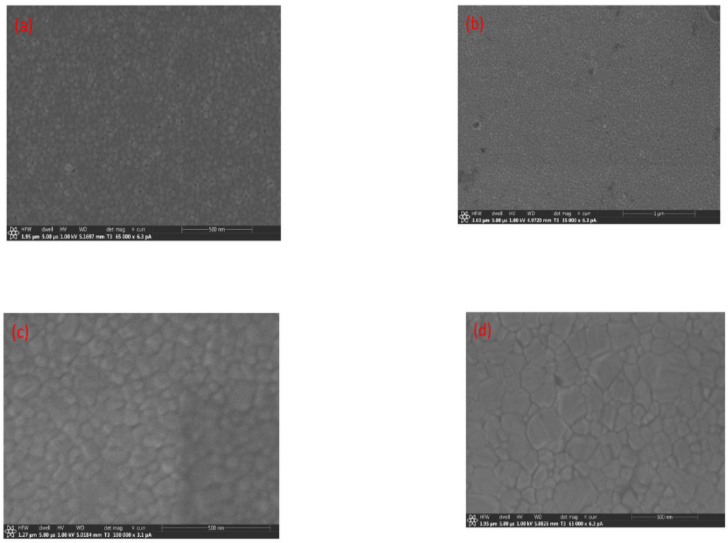

Fig. 6. Surface morphology of NCoZF films annealed at (a) 500ºC (b) 600ºC(c) 700ºC and (d) 800ºC

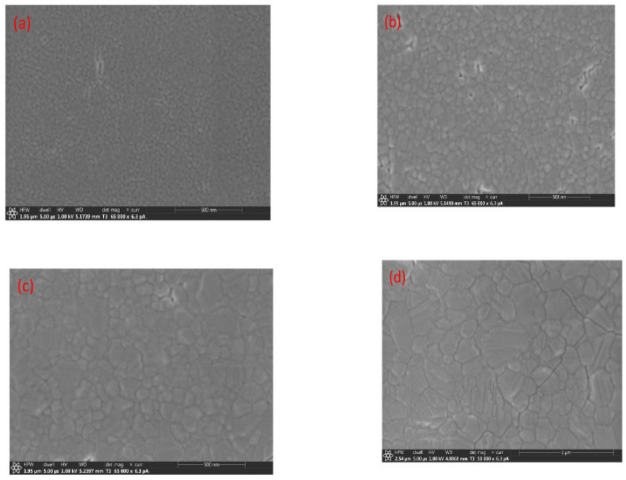

Fig. 7. Surface morphology for NCuZF films annealed at (a) 500ºC (b) 600ºC(c) 700ºC and (d) 800ºC

Table II: Grain size of NZF, NCoZF and NCuZF films annealed at different temperature

Sample	**Grain size(nm)**			
	500 °C	**600 °C**	**700 °C**	**800 °C**
NZF	34	47.6	84.6	128.54
NCoZF	29	37.5	54	183
NCuZF	19.5	49	85	214

To further understand the effect of annealing temperature on the magnetic properties, the grain size distribution of all the films was investigated. Figures 5, 6 and 7 are the SEM micrographs obtained on NZF, NCoZF and NCuZF films annealed at 500, 600, 700 and 800 °C. The grain size for all the films annealed at various temperatures are summarized in Table II. The values reported for each sample were obtained by averaging the measured diameter of approximately 6-8 grains.

It was observed that temperature has a significant effect on the grain size of these films. As the annealing temperature increases, the grain size also increases but nonlinearly. This trend was observed for all the samples. As smaller grains have higher surface energy compared to larger grains, smaller grains diffuse into larger grains to minimize the total energy. As a result, grain boundary moves, the larger grains keep growing at the expense of smaller grains which eventually vanish [34]. It was observed that with the increase in the annealing temperature, the grain size becomes larger, but many cracks developed on the surface of the films annealed at higher temperatures. No crack formation was observed from samples which were annealed at temperature upto 600 ºC whereas the cracks started developing when annealing temperature was above 700 ºC. This behavior was consistent for the three types of films. More cracks were seen on films annealed at 800ºC in comparison to those annealed at 700ºC. Representative SEM micrographs for NZF and NCuZF films annealed at 800 ºC are shown in Figure 8 (a, b).

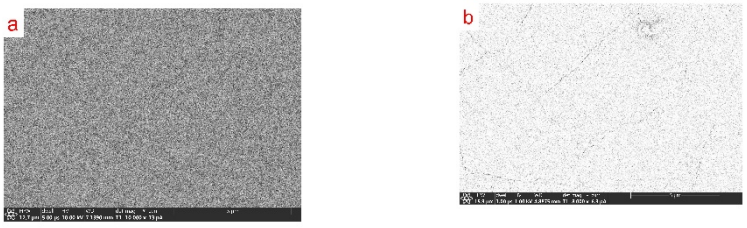

Fig. 8. Micrographs showing crack formation on films annealed at 800ºC for (a) NZF and (b) NCuZF

Slonczewski et al reported that cracks severely perturb the domain structure in their immediate vicinity [36] which results in a higher demagnetization factor with respect to the original film [37]. In our case, only those films which were annealed at 700 and 800 ºC developed cracks. This could be the reason for the reduction of the saturation magnetization from such films. The interdiffusion of the film and substrate is also reported to be another reason for the degradation

of the saturation magnetization [38]. In this work, all the films were prepared on Si/SiO_2 which should prevent interdiffusion. Further, evaporation of volatile Zn is also reported to play a role in the reduction of saturation magnetization of the films as the volatilization of Zn^{2+} leads to lattice defects [38,39]. However, for our films the amount of Zn did not vary drastically, irrespective of annealing temperature, which was verified by Energy Dispersive Spectroscopy.

To evaluate the effect of doping on the magnetic properties, the in-plane magnetic hysteresis loops of the NZF, NCoZF and NCuZF films annealed at 600 °C are presented in Figure 9. These loops are indicative of typical behavior of soft ferrite. It is clear that all the samples are magnetized to saturation when the external field is less than 5,000 Oe. The NZF film exhibit highest saturation magnetization value followed by films doped with Co. Cu doped film has the lowest saturation magnetization value. The coercivity of the in-plane hysteresis loop of NZF, NCoZF and NCuZF films annealed at 600°C are 102 Oe, 509 Oe and 95Oe, respectively. Thus, doping $Ni_{0.5}Zn_{0.5}Fe_2O_4$ films with $Co_{0.2}$ resulted in a large increase in the coercivity whereas doping with $Cu_{0.2}$ decreased the coercivity. A similar trend has been reported by Kumar et al for Co doped and Xiang et al for Cu doped NiZF films [26,40].

Among various factors, the cation distribution, structure, and composition play a significant role in the magnetic properties for spinel ferrites [41]. The variation of saturation magnetization can be estimated using the exchange interaction of the ions in the tetrahedral (A) and octahedral (B) sites [42]. Some ions tend to have special preference to a certain site based on the environment. For example, Zn^{2+} prefers tetrahedral (A) site due to the electronic configuration being favorable for tetrahedral bonding to the oxygen ions [43]. Even though Zn^{2+} and Co^{2+} have the same ionic radius, Co tends to move to octahedral (B) site because of its configuration [43].

On the other hand, Ni^{2+} and Cu^{2+} have strong preference for octahedral (B) site [43,44] . Iron cation can be distributed to both sites with the preference to move to octahedral (B) site [42].

For NZF films, the saturation magnetization may be attributed to the Ni and Zn concentration in the spinel lattice. Zn^{2+} occupy tetrahedral (A) site and Ni^{2+} occupy octahedral (B) site. Fe^{3+} can migrate from A to B site to accommodate Zn^{2+}.However, Fe^{3+} can still exist on A site. The Fe^{3+} moments on the tetrahedral (A) site orient all the octahedral (B) site moments antiparallel to them so that Fe^{3+} moments from the A site are neutralized. Thus, the uncompensated moments result in net magnetic moments [5,45]. According to Miller's site preference energies of ions [46], the cations distribution of NZF film can be written as follows:

$$(Zn_{0.5}Fe_{0.5})\ (A\ site)\ [Ni_{0.5}Fe_{1.5}]O_4\ (B\ site)$$

According to Néel model, the magnetic moment of $Ni_{0.5}Zn_{0.5}Fe_2O_4$ ferrite film can be calculated using the following equation: $M=|M_B-M_A|$, where M_A and M_B are the magnetic moments in the A and B site [27,29]. Using this equation and the values of magnetic moments of Zn^{2+}, Ni^{2+}, Cu^{2+}, Co^{2+} and Fe^{3+} ions as 0, 2, 1, 3 and 5 μ_B, respectively, the net magnetic moment values of NZF, NCoZF, and NCuZF films were calculated as 6, 5.8 and 5.4 μ_B respectively. The trend of our experimental results for magnetization are in agreement with the calculations.

The increase in coercivity value can also be related to the grain size. The coercivity increases until a critical diameter of the grain size is reached, which acts as a single domain. The smaller the grain size, the lower the value of coercivity due to the randomizing effects of thermal energy. Thermal energy plays an important role in magnetic instability in single domain. As the grain size is small, thermal agitation will be small. As a result, there will be fewer fluctuations in the magnetic spin orientations [47]. On the other hand, the increase of annealing temperature

increases the grains size, which reduces the grain boundary volume. According to Juang and Wohlfarth, increasing grain size results in multi-domain grain structures which ultimately results in the reduction in coercivity [48,49]. The reason is the domain wall in large multi-domain grains can easily be shifted by a relatively weak magnetic field [49] . Fernando et al. also showed a linear inverse proportionality between coercivity (H_c) and grain size (D) given by H_c α $1/D$[50]. Murali et. al. calculated the critical size of the mono-domain (D_m) to be 50.2 nm for NiZn ferrite which is comparable with our result [49]. The grain size of the films annealed at 600 ºC could be less than the critical diameter of the grain size and could be attributed as a reason for seeing highest value of coercivity from such films.

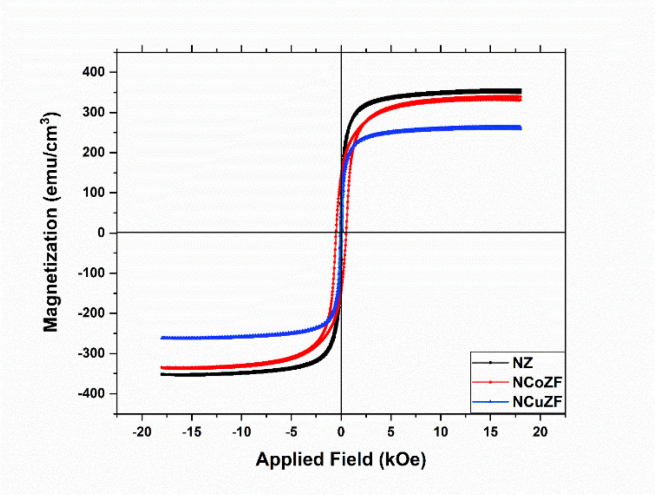

Fig. 9. In plane magnetization of NZF, NCoZF, and NCuZF films

4. **Conclusion:**

Thin films of $Ni_{0.5}Zn_{0.5}Fe_2O_4$, $Ni_{0.35}Co_{0.2}Zn_{0.45}Fe_2O_4$ and $Ni_{0.35}Cu_{0.2}Zn_{0.45}Fe_2O_4$ were successfully prepared by sol gel method. NZF films showed maximum saturation magnetization followed by NCoZF films, whereas NCuZF films showed minimum saturation magnetization. Doping NZF films with Co resulted in increase in the coercivity whereas doping NZF films with

Cu resulted in decrease in the coercivity, in comparison to NZF films. Annealing temperature was seen to affect the structural and magnetic properties of the films. Even though highest grain size was obtained from films annealed at 800 ºC, the highest magnetization and coercivity values were obtained from films annealed at 600 ºC temperature. Based on the requirement of a specific application, magnetic properties of these films can be tuned by doping with a suitable dopant.

ACKNOWLEDGMENTS

This material is based upon work supported by the National Science Foundation under Grant No. 1708690. Any opinions, findings and conclusions or recommendations expressed in this material are those of the author(s) and do not necessarily reflect the views of the National Science Foundation. The authors acknowledge the Central Analytical Facility (CAF) UA for use of characterization facilities.

List of References:

[1] J. Prado, M.E. Gómez, P. Prieto, A. Mendoza, Growth temperature dependence of the hysteretic behavior of Ni0.5Zn0.5Fe2O4 thin films, J. Magn. Magn. Mater. 321 (2009) 2792–2794. https://doi.org/10.1016/j.jmmm.2009.04.015.

[2] J. Gao, Y. Cui, Z. Yang, The magnetic properties of NixZn1-xFe 2O4 films fabricated by alternative sputtering technology, Mater. Sci. Eng. B Solid-State Mater. Adv. Technol. 110 (2004) 111–114. https://doi.org/10.1016/j.mseb.2003.10.111.

[3] Z. Beji, S. Ammar, L.S. Smiri, M.J. Vaulay, F. Herbst, B. Gallas, F. Fívet, Spray deposition of nanocrystalline Ni1-x Znx Fe2 O4 ($x \leq 0.6$) films from polyol-mediated sol: Microstructure and magnetic properties, J. Appl. Phys. 103 (2008) 1–4. https://doi.org/10.1063/1.2843742.

[4] J.L. Dormann, M. Nogues, Magnetic structures in substituted ferrites, J. Phys. Condens. Matter. 2 (1990) 1223–1237. https://doi.org/10.1088/0953-8984/2/5/014.

[5] I.Z. Rahman, T.T. Ahmed, L. Powell, Magnetic and physical characterization of nano granular Ni-Zn-Cu based ferrite powders, J. Metastable Nanocrystalline Mater. 17 (2003) 9–16. https://doi.org/10.4028/www.scientific.net/JMNM.17.9.

[6] G. Dixit, J.P. Singh, R.C. Srivastava, H.M. Agrawal, R.J. Choudhary, A. Guptab, Annealing effect on the structural andmagnetic properties of nickel ferrite thin films, Surf. Interface Anal. 42 (2010) 151–156. https://doi.org/10.1002/sia.3195.

[7] M. Kaiser, Effect of nickel substitutions on some properties of Cu-Zn ferrites, J. Alloys Compd. 468 (2009) 15–21. https://doi.org/10.1016/j.jallcom.2008.01.070.

[8] Z. Yue, J. Zhou, Z. Gui, L. Li, Magnetic and electrical properties of low-temperature sintered Mn-doped NiCuZn ferrites, J. Magn. Magn. Mater. 264 (2003) 258–263. https://doi.org/10.1016/S0304-8853(03)00214-2.

[9] H. Su, H. Zhang, X. Tang, Y. Jing, Y. Liu, Effects of composition and sintering temperature on properties of NiZn and NiCuZn ferrites, J. Magn. Magn. Mater. 310 (2007) 17–21. https://doi.org/10.1016/j.jmmm.2006.07.022.

[10] M. Ušáková, J. Lukáč, R. Dosoudil, V. Jančárik, A. Grusková, E. Ušák, J. Sláma, J. Šubrt, Influence of Cu 2+ ions on structural and magnetic properties of NiZn ferrites, J. Mater. Sci. Mater. Electron. 18 (2007) 1183–1189. https://doi.org/10.1007/s10854-007-9347-9.

[11] J. Mürbe, J. Töpfer, Ni-Cu-Zn Ferrites for low temperature firing: II. Effects of powder morphology and Bi2O3 addition on microstructure and permeability, J. Electroceramics. 16 (2006) 199–205. https://doi.org/10.1007/s10832-006-6362-9.

[12] K.S. Park, J.H. Nam, J.H. Oh, Magnetic properties of NiCuZn ferrites with addition of tungsten trioxide, J. Magn. Magn. Mater. 226–230 (2001) 1415–1417. https://doi.org/10.1016/S0304-8853(01)00028-2.

[13] K. Sun, Z. Lan, Z. Yu, L. Li, J. Huang, Grain growth and magnetic properties of Nb2O5-doped NiZn ferrites, Jpn. J. Appl. Phys. 47 (2008) 7871–7875. https://doi.org/10.1143/JJAP.47.7871.

[14] C.M. Fu, H.S. Hsu, Y.C. Chao, N. Matsushita, M. Abe, High-frequency transport properties of spin-spray plated Ni-Zn ferrite thin films, J. Appl. Phys. 93 (2003) 7127–7129. https://doi.org/10.1063/1.1558197.

[15] A. Fujiwara, M. Tada, T. Nakagawa, M. Abe, Permeability and electric resistivity of spin-sprayed Zn ferrite films for high-frequency device applications, J. Magn. Magn. Mater. 320 (2008) 2007–2009. https://doi.org/10.1016/j.jmmm.2007.11.026.

[16] M. Desai, S. Prasad, N. Venkataramani, I. Samajdar, A.K. Nigam, N. Keller, R. Krishnan, E.M. Baggio-Saitovitch, B.R. Pujada, A. Rossi, Anomalous variation of coercivity with annealing in nanocrystalline NiZn ferrite films, J. Appl. Phys. 91 (2002) 7592–7594. https://doi.org/10.1063/1.1447504.

[17] K. Sun, Y. Dai, Y. Yang, Z. Yu, H. Liu, X. Jiang, Z. Lan, Influence of substrate type on the property of nickle–zinc ferrite thin films, Ceram. Int. 42 (2016) 3028–3032. https://doi.org/10.1016/j.ceramint.2015.10.089.

[18] Y. Liu, Y. Li, H. Zhang, D. Chen, C. Mu, Structural and magnetic properties of NiZn-ferrite thin films prepared by radio frequency magnetron sputtering, J. Appl. Phys. 109 (2011) 6–9. https://doi.org/10.1063/1.3556775.

[19] R. Xu, L.S. Wang, X.L. Liu, M. Lei, H.Z. Guo, Y. Chen, J.B. Wang, D.L. Peng, Influence of substrate temperature on high-frequency soft magnetic properties of [Fe80Ni20-O/NiZn-ferrite]n multilayer thin films, J. Alloys Compd. 604 (2014) 43–49. https://doi.org/10.1016/j.jallcom.2014.03.099.

[20] H. Itoh, T. Uemura, H. Yamaguchi, S. Naka, Chemical vapour deposition of epitaxial Ni-Zn ferrite films by thermal decomposition of acetylacetonato complexes, J. Mater. Sci. 24 (1989) 3549–3552. https://doi.org/10.1007/BF02385738.

[21] G.R. Pulliam, Chemical vapor growth of single-crystal magnetic oxide films, J. Appl. Phys. 38 (1967) 1120–1126. https://doi.org/10.1063/1.1709508.

[22] D. Ravinder, K. Vijay Kumar, A. V. Ramana Reddy, Preparation and magnetic properties of Ni-Zn ferrite thin films, Mater. Lett. 57 (2003) 4162–4164. https://doi.org/10.1016/S0167-577X(03)00091-0.

[23] C.S. Pawar, M.P. Gujar, V.L. Mathe, Optical Properties of Spin-Deposited Nanocrystalline Ni-Zn Ferrite Thin Films Processed by Sol-Gel, J. Supercond. Nov. Magn. 30 (2017) 615–625. https://doi.org/10.1007/s10948-016-3720-y.

[24] J.G. Lee, J.Y. Park, Y.J. Oh, C.S. Kim, Magnetic properties of CoFe2O4 thin films prepared by a sol-gel method, J. Appl. Phys. 84 (1998) 2801–2804. https://doi.org/10.1063/1.368393.

[25] S. Zahi, M. Hashim, A.R. Daud, Synthesis, magnetic properties and microstructure of Ni-Zn ferrite by sol-gel technique, J. Magn. Magn. Mater. 308 (2007) 177–182. https://doi.org/10.1016/j.jmmm.2006.05.033.

[26] J. Xiang, X. Shen, F. Song, M. Liu, One-dimensional NiCuZn ferrite nanostructures: Fabrication, structure, and magnetic properties, J. Solid State Chem. 183 (2010) 1239–1244. https://doi.org/10.1016/j.jssc.2010.03.041.

[27] L. Li, L. Peng, X. Zhu, D. Yang, Effects of Cu and Co Substitution on the Properties of NiZn Ferrite Thin Films, 10 (2012) 88–92.

[28] F. Liu, C. Yang, T. Ren, A.Z. Wang, J. Yu, L. Liu, NiCuZn ferrite thin films grown by a sol-gel method and rapid thermal annealing, J. Magn. Magn. Mater. 309 (2007) 75–79. https://doi.org/10.1016/j.jmmm.2006.06.014.

[29] L. Li, L. Peng, Y. Li, X. Zhu, Structure and magnetic properties of Co-substituted NiZn

ferrite thin films synthesized by the solgel process, J. Magn. Magn. Mater. 324 (2012) 60–62. https://doi.org/10.1016/j.jmmm.2011.07.039.

[30] A.R. Chavan, M. V. Shisode, P.G. Undre, K.M. Jadhav, Influence of Cr3+ substitution on structural, morphological, optical, and magnetic properties of nickel ferrite thin films, Appl. Phys. A Mater. Sci. Process. 125 (2019) 1–9. https://doi.org/10.1007/s00339-019-2768-5.

[31] K. Sun, Z. Lan, Z. Yu, X. Nie, L. Li, C. Liu, Magnetic properties of Sn-substituted NiZn ferrite thin films, J. Magn. Magn. Mater. 320 (2008) 1180–1183. https://doi.org/10.1016/j.jmmm.2007.11.005.

[32] Z. Qian, G. Wang, J.M. Sivertsen, J.H. Judy, NiZn Ferrite, 33 (1997) 3748–3750.

[33] A.A. Rodríguez-Rodríguez, O.S. Rodríguez-Fernández, J.G. Osuna-Alarcó, S.M. Montemayor, Synthesis of multielement ferrites and their silica composites, J. Sol-Gel Sci. Technol. 61 (2012) 534–540. https://doi.org/10.1007/s10971-011-2656-8.

[34] J. Li, Z. Yu, K. Sun, X. Jiang, Z. Xu, Z. Lan, Grain growth kinetics and magnetic properties of NiZn ferrite thin films, J. Alloys Compd. 513 (2012) 606–609. https://doi.org/10.1016/j.jallcom.2011.11.022.

[35] S.Y. Bae, C.S. Kim, Y.J. oh, Magnetic properties of sol-gel derived Ni–Zn ferrite thin films on yttria stabilized zirconia buffered Si(100), J. Appl. Phys. 85 (1999) 5226–5228. https://doi.org/10.1063/1.369951.

[36] J. Slonczewski, B. Argyle, J. Spreen, Domain-wall vibrations, M (1981) 2760–2765.

[37] C.S. Smith, K. Sondhi, Z.H. Fan, T. Nishida, D.P. Arnold, Effect of Mechanical Cycling

on the Magnetic Properties of Permalloy Films Electroplated on Stretchable Substrates, 2019 IEEE Int. Flex. Electron. Technol. Conf. IFETC 2019. (2019) 2019–2021. https://doi.org/10.1109/IFETC46817.2019.9073710.

[38] S.Y. Bae, H.J. Jung, C.S. Kim, Y.J. Oh, Magnetic properties of sol-gel derived Ni-Zn ferrite thin films, J. Phys. IV JP. 8 (1998) 2–5. https://doi.org/10.1051/jp4:1998262.

[39] L. Sun, J. Guo, Q. Ni, E. Cao, Y. Zhang, W. Hao, L. Ju, Effect of Zn2+ doping on the structural, magnetic and dielectric properties of MnFe2O4 prepared by the sol–gel method, J. Mater. Sci. Mater. Electron. 29 (2018) 5356–5362. https://doi.org/10.1007/s10854-017-8501-2.

[40] R. Kumar, H. Kumar, R.R. Singh, P.B. Barman, Variation in magnetic and structural properties of Co-doped Ni–Zn ferrite nanoparticles: a different aspect, J. Sol-Gel Sci. Technol. 78 (2016) 566–575. https://doi.org/10.1007/s10971-016-3984-5.

[41] Y. Li, X. Liu, X. Kan, S. Feng, Q. Lv, J. Huang, J. Zhao, J. Hu, Investigation of structural and magnetic properties of Cu-substituted NiZn spinel ferrites, J. Mater. Sci. Mater. Electron. 31 (2020) 17133–17142. https://doi.org/10.1007/s10854-020-04273-y.

[42] A. Ghasemi, E. Ghasemi, E. Paimozd, Influence of copper cations on the magnetic properties of NiCuZn ferrite nanoparticles, J. Magn. Magn. Mater. 323 (2011) 1541–1545. https://doi.org/10.1016/j.jmmm.2011.01.014.

[43] T.T. Ahmed, I.Z. Rahman, M.A. Rahman, Study on the properties of the copper substituted NiZn ferrites, J. Mater. Process. Technol. 153–154 (2004) 797–803. https://doi.org/10.1016/j.jmatprotec.2004.04.188.

[44] A. Tawfik, Jump rate and linear distance of vacancy on the structure and electrical conductivity of Ni0.65Zn0.35CuxFe2-xO4 ferrites, J. Magn. Magn. Mater. 224 (2001) 197–200. https://doi.org/10.1016/S0304-8853(00)00589-8.

[45] A.E. Saba, E.M. Elsayed, M.M. Moharam, M.M. Rashad, R.M. Abou-Shahba, Structure and magnetic properties of Ni x Zn1-x Fe2O4 thin films prepared through electrodeposition method, J. Mater. Sci. 46 (2011) 3574–3582. https://doi.org/10.1007/s10853-011-5271-8.

[46] A. Miller, Distribution of Cations in Spinels, J. Appl. Phys. 30 (1959) S24–S25. https://doi.org/10.1063/1.2185913.

[47] Y. Yusuf, R.S. Azis, S. Kanagesan, G. Bahmanrokh, Microstructure and magnetic properties of Ni-Zn ferrite thin film synthesized using sol-gel and spin-coating technique, J. Aust. Ceram. Soc. 53 (2017) 767–774. https://doi.org/10.1007/s41779-017-0090-2.

[48] D.S. Mathew, R.S. Juang, An overview of the structure and magnetism of spinel ferrite nanoparticles and their synthesis in microemulsions, Chem. Eng. J. 129 (2007) 51–65. https://doi.org/10.1016/j.cej.2006.11.001.

[49] M. Bissannagari, J. Kim, Inkjet printing of NiZn-ferrite films and their magnetic properties, Ceram. Int. 41 (2015) 8023–8027. https://doi.org/10.1016/j.ceramint.2015.02.151.

[50] F.J.G. Landgraf, J.R.F. Da Silveira, D. Rodrigues-Jr., Determining the effect of grain size and maximum induction upon coercive field of electrical steels, J. Magn. Magn. Mater. 323 (2011) 2335–2339. https://doi.org/10.1016/j.jmmm.2011.03.034.